IEEE Access
Multidisciplinary | Rapid Review | Open Access Journal

Received May 13, 2020, accepted May 23, 2020, date of publication May 26, 2020, date of current version June 4, 2020.

Digital Object Identifier 10.1109/ACCESS.2020.2997820

Hybrid WDM FSO Fiber Access Network With Rayleigh Backscattering Noise Mitigation

CHIEN-HUNG YEH[1], JHAO-REN CHEN[1], WEI-YAO YOU[1], AND CHI-WAI CHOW[2,3], (Senior Member, IEEE)

[1]Department of Photonics, Feng Chia University, Taichung 40724, Taiwan
[2]Department of Photonics, National Chiao Tung University, Hsinchu 30010, Taiwan
[3]Institute of Electro-Optical Engineering, National Chiao Tung University, Hsinchu 30010, Taiwan

Corresponding authors: Chien-Hung Yeh (yeh1974@gmail.com) and Chi-Wai Chow (cwchow@faculty.nctu.edu.tw)

This work was supported by the Ministry of Science and Technology, Taiwan, under Grant MOST-108-2221-E-035-072.

ABSTRACT In the paper, we present and investigate an integrated wavelength-division-multiplexing (WDM) free space optical (FSO) fiber access network for 51 km long-reach connection. Here, the proposed network architecture also can mitigate Rayleigh backscattering (RB) interferometric beat noise. We employ symmetric 4 × 10 Gbit/s on-off keying (OOK) WDM-FSO downstream and upstream wavelengths for demonstration. According to the simulated and experimental results, the free space transmission length of 400 to 940 m can be achieved based on various WDM-FSO downstream signals and their corresponding power budget, when the wavelengths are without optical amplification.

INDEX TERMS Free space optical (FSO) communication, passive optical network (PON), wavelength-division-multiplexing (WDM), Rayleigh backscattering (RB) noise mitigation, long-reach, on-off keying.

I. INTRODUCTION

Due to the rapid growth of broadband requirement, such as cloud radio access network (C-RAN), big data, internet, and video service, the integrated fiber-optics communication and high-speed wireless access network would be the better candidate for supporting the future scenario of broadband everywhere [1]–[4]. In recent times, the capacity requirements of passive optical networks (PONs) for the fiber to the home (FTTH) are extended from 2.5 to 40 Gbit/s or even 100 Gbit/s, such as using time-division-multiplexing (TDM) [5], [6], wavelength-division-multiplexing (WDM) [7], [8] and time and wavelength-division-multiplexing (TWDM) access techniques [9], [10]. Furthermore, the fiber based PON networks also can be exploited to provide the backhaul and fronthaul connection for the millimeter wave (MMW) and free space optical (FSO) communications [11], [12]. Owing to some special geographical or environmental restrictions, the fiber lines cannot be provisioned and connected for signal connection in PON system [13]. Thus, using the integrated FSO and MMW signals in PON access could solve the problem via wireless channel transmission [14], [15].

The WDM-PON system would also bring the Rayleigh backscattering (RB) interferometric beat noise [16], when the same wavelengths were utilized for downstream and upstream connections. To avoid the RB problem in WDM-PON network, utilizing the advanced signal modulations [17], matchless fiber network architecture [18] and dual-band wavelengths [19] have been demonstrated.

In this work, we propose and investigate a WDM-FSO PON architecture together with RB noise alleviation to provide the fiber signal and FSO traffic simultaneously for prove of concept. In the experiment, 4 × 10 Gbit/s on-off keying (OOK) downstream (λ_1 to λ_4) and upstream (λ_2 to λ_5) signals are employed for 51 km long-reach fiber connection in PON access. In the presented network, some WDM wavelengths can be received in each corresponding optical network unit (ONU) directly through fiber connection. The others may integrate the FSO link in PON architecture to overcome the environmental restraint. Based on our experimental and simulated results, the FSO transmission length of 400 to 940 m can be reached depending on different WDM wavelengths and their related power budget after 51 km fiber link without signal amplification. In this demonstration, if we want to achieve a longer free space transmission length, an optical amplifier may be required to apply in the corresponding optical wireless unit (OWU) for enhancing the power budget.

The associate editor coordinating the review of this manuscript and approving it for publication was Nicola Andriolli.

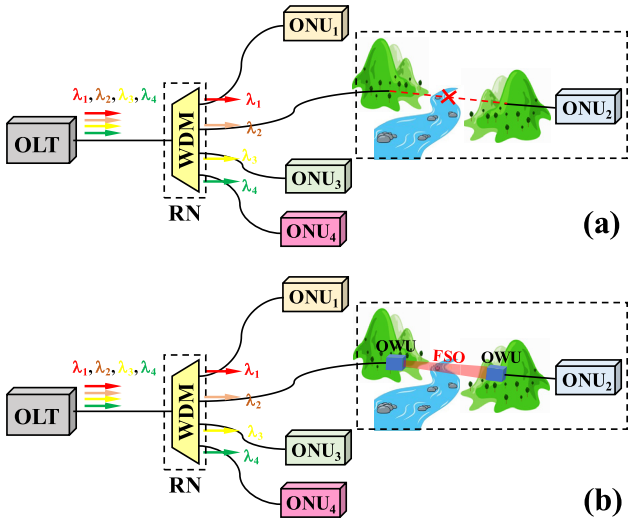

FIGURE 1. (a) Conventional WDM-PON architecture. (b) Hybrid WDM and FSO PON system. OLT: optical line terminal; WDM: wavelength-division-multiplexing; RN: remote node; ONU: optical network unit; OWU: optical wireless unit; FSO: free space optical communication.

II. EXPERIMENT AND RESULTS

Fig. 1(a) exhibits the scenario of conventional WDM-PON system for point-to-point (PtP) data access. Each ONU would receive the corresponding wavelength for signal transmission. However, due to some special environment limits, the fiber may be not connected between the wider rivers and two mountains or other, as shown in Fig. 1(a). To solve the disconnection in the such PON network, using the FSO technology, which could be integrated in WDM-PON, may be the better solution. As illustrated in Fig. 1(b), we can utilize two optical wireless units (OWUs) between the OLT and ONU according to the geographical feature for delivering wireless downstream FSO signal for data connection. Then, the FSO signal would launch into the corresponding ONU after a period of free space transmission. Therefore, the FSO access can support the bidirectional signal transmission in WDM-PON system to overcome the environmental restriction.

Fig. 2 presents the proposed hybrid and bidirectional WDM and FSO PON architecture for prove of concept. In the OLT, each laser diode (LD) with different output wavelength is exploited to regard as the downstream WDM channels. Each LD connects to the polarization controller (PC), Mach-Zehnder modulator (MZM) and 3-port optical circulator (OC). Here, the WDM downstream wavelengths of λ_1 to λ_N would leave the $2 \times N$ WDM multiplexer through the "a" port, as plotted in Fig. 2. The WDM downstream wavelengths will pass through the OC, single-mode fiber (SMF_1) and the remote node (RN). Then, the WDM wavelengths can be divided via the $2 \times N$ WDM multiplexer in the RN. Through a length of SMF_2 link, the downstream wavelength could transfer to wireless FSO signal by the OC and fiber-based collimator (FC) in the optical wireless unit (OWU), as exhibited in Fig. 2. Next, the downstream FSO also can be received through the focusing lens and FC in the other OWU after wireless FSO link. Finally, the FSO wavelength can enter the corresponding ONU for downstream demodulation through a SMF_3 transmission. In addition, the upstream modulation data is also applied on the MZM in the ONU for upstream traffic. The upstream signal of λ_2 to λ_{N+1} can transmit through the optical coupler (CP), SMF_3, SMF_2, WDM multiplexer, OC and SMF_1, and then into the OLT for decoding, as seen in Fig. 2. In general, the WDM multiplexer could be utilized with standard channel in the available range of C- or L-bands. Moreover, the insertion losses of WDM multiplexer, CP and OC are 6, 3 and 1 dB, respectively.

As we know, the RB beat noise in WDM-PON network would affect the signal performances, while the same wavelengths are applied for transmission [20]. The proposed hybrid WDM and FSO PON system also can mitigate the RB noise. Here, we can apply the $2 \times N$ WDM multiplexer in the OLT and RN for bidirectional data traffics. To realize the operation mechanism of the designed PON network, the 2×4 WDM multiplexer can be used for demonstration. Fig. 3 indicates the optical output characteristic of 2×4 WDM multiplexer. As illustrated in Fig. 3, the WDM wavelengths of λ_1 to λ_N and λ_2 to λ_{N+1} can pass through the WDM multiplexer from the input/output ports of "a" and "b", respectively. Hence, the output/input ports of "1" to "4" could allow the wavelengths of λ_1 and λ_2, λ_2 and λ_3, λ_3 and λ_4, and λ_4 and λ_5 for passing, respectively. Due to the periodic wavelength arrangement of 2×4 WDM multiplexer, the output/input ports of "1" to "4" could also permit the wavelengths of λ_5 and λ_6, λ_6 and λ_7, λ_7 and λ_8, and λ_8 and λ_9, respectively, as seen in Fig. 3. Here, the downstream and upstream wavelengths of λ_1 and λ_2, λ_2 and λ_3, λ_3 and λ_4, and λ_4 and λ_5 are applied in the demonstration, respectively. Hence, according to the designed WDM architecture, we exploit the downstream and upstream signals with various wavelengths to avoid the RB interferometric noise, as exhibited in Fig. 2.

Fig. 4 presents the experimental setup of the downstream and upstream FSO transmission configuration, respectively. To demonstrate WDM signal transmission in the presented PON network, five wavelengths of 1530.33, 1534.25, 1538.19, 1542.14 and 1546.12 nm are exploited to regard as the downstream and upstream traffics, respectively, for prove of concept. However, the standard WDM wavelengths with fixed channel spacing would be the better choice for practical signal connection. In the experiment, we utilize a tunable laser source (TLS, produced by *General Photonics*) to regard as the WDM wavelength for selecting. The output power and optical signal to noise ratio (OSNR) of TLS are 13 dBm and >50 dB over the tuning range of 1528.77 to 1563.86 nm. In the downstream measurement, 10 Gbit/s on-off keying (OOK) modulation signal with pattern length of $2^{15}-1$ is applied on the 10 GHz MZM with 6 dB insertion loss. The MZM could be operated over C-band wavelength range.

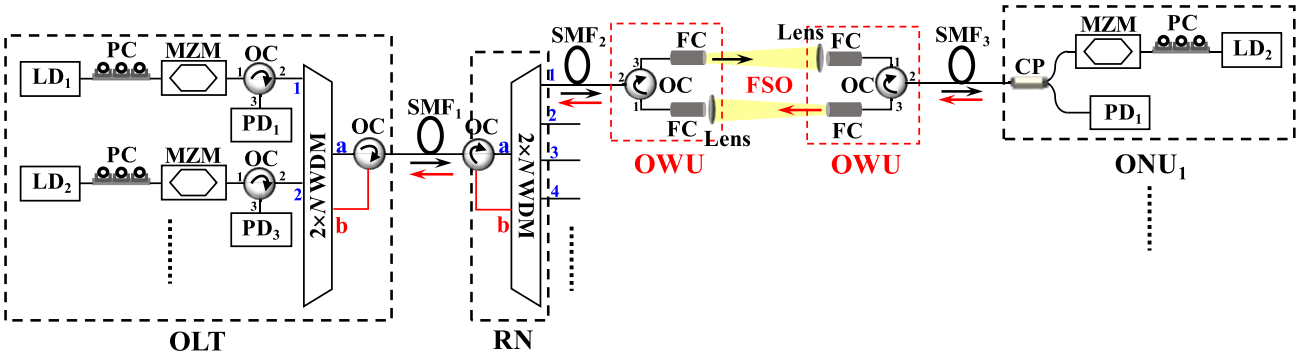

FIGURE 2. Proposed hybrid WDM FSO PON architecture with RB beat noise mitigation.

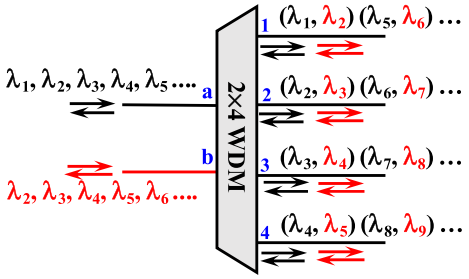

FIGURE 3. The periodic output characteristic of 2 × 4 WDM multiplexer.

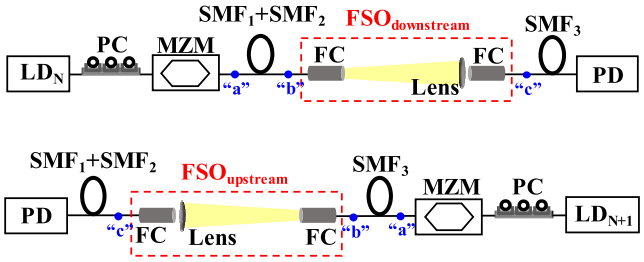

FIGURE 4. Experimental setups for downstream and upstream WDM-FSO transmissions.

To achieve the optimal output power, the PC is adjusted properly. The operation bandwidth of PC is from 1260 to 1650 nm. Here, the output power of each downstream wavelength is set at 7.5 dBm at the "a" point, as seen in Fig. 4. The $SMF_1 + SMF_2$ and SMF_3 (Corning SMF-28e, attenuation = 0.2 dB/km) transmission lengths of 26 and 25 km, and 50 and 1 km are utilized, respectively, for measurement. To receive the downstream and upstream FSO signals, 10 GHz PIN based PD is exploited for decoding.

In the measurement, the divergence angle, focal length, and diameter of each FC is 0.016°, 37.13 mm and 20 mm, respectively. The available bandwidth of FC is 1050 to 1620 nm. The diameter and focal length of 50.4 mm and 75 mm is chosen for the focusing lens. The lens is unmounted achromatic doublet with AR coating over the range of 1050 to 1700 nm. The gap between the focusing lens and FC is around 45 mm. Between two OWUs, two FCs and a focusing lens are applied for the FSO connection. The coupling loss of ∼2.6 dB can be measured between the "b" and "c" locations through 2 m wireless FSO connections without the atmospheric interference of fog, rain, and turbulence etc. In addition, higher modulation rate would reduce the obtained power sensitivity after a length of SMF transmission due to the fiber chromatic dispersion. The used 10 GHz MZM has negative chirp of −0.7 in the demonstration. Hence, the fiber dispersion could be pre-compensated to enhance the BER performance of WDM signal.

Fig. 5(a) plots the observed bit error rate (BER) performance of downstream WDM-FSO signal at the wavelengths of 1530.33 (λ_1), 1534.25 (λ_2), 1538.19 (λ_3) and 1542.14 nm (λ_4), when the $SMF_1 + SMF_2$, SMF_3 and free space transmission length are 26 km, 25 km and 2 m, respectively. The corresponding optical sensitivities of the four wavelengths are measured at −25, −24, −20 and −21 dBm under the error free status (BER $\leq 1 \times 10^{-9}$) respectively, as displayed in Fig. 5(a). Moreover, the power sensitivities of −32.5, −31, −27 and −27 dBm are also observed below the forward error correction (FEC) level (BER $\leq 3.8 \times 10^{-3}$). Hence, as moving toward the longer wavelength slowly, the obtained power sensitivity will also become higher, as also seen in Fig. 5(a).

Fig. 5(b) presents the detected BER measurement of upstream WDM-FSO signal, while the four wavelengths are 1534.25 (λ_2), 1538.19 (λ_3), 1542.14 (λ_4) and 1546.12 nm (λ_5), respectively. Here, the attained power sensitivities are −24, −21, −20 and −20.5 dBm under the error free level, respectively. Moreover, to meet the FEC target, the corresponding sensitivities of four upstream wavelengths are −31, −26.5, −27 and −26.5 dBm, respectively. As a result, the total power budgets of four downstream and upstream wavelengths are calculated at 39, 38.5, 34.5 and 34.5 dB and 38.5, 34, 34.5 and 34 dB under the FEC threshold, respectively. Due to the downstream and upstream traffics with different wavelengths in the proposed WDM-FSO PON, the RB noise effect can be ignored completely.

Then, we change the fiber distance of $SMF_1 + SMF_2$ and SMF_3 to 50 and 1 km in the experimental setup. The free space link length of 2 m is also maintained. Thus, Fig. 6(a) display the observed BER characteristics of four downstream

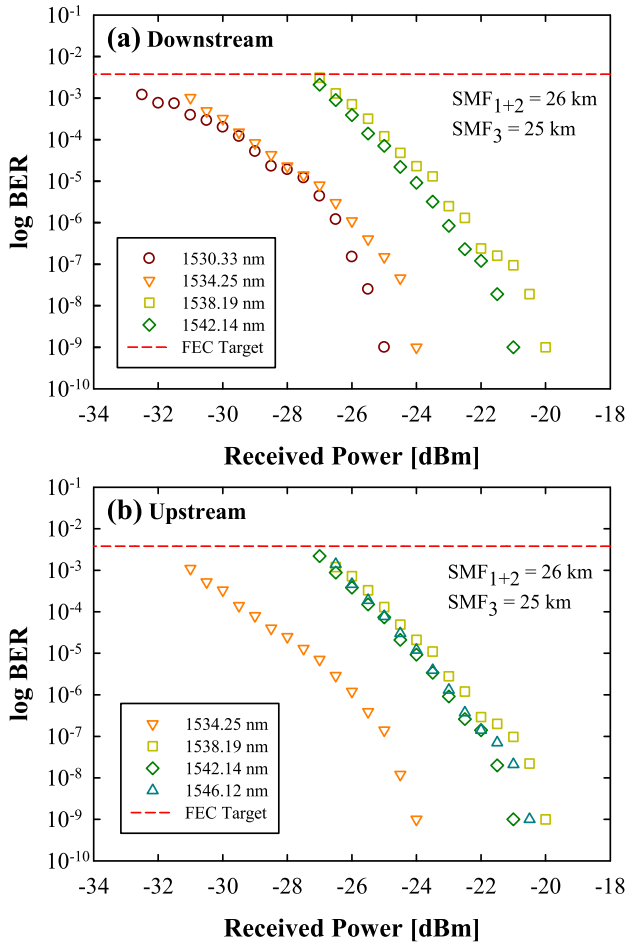

FIGURE 5. Obtained BER performances of four WDM (a) downstream and (b) upstream signals through 26 km $SMF_1 + SMF_2$, 25 km SMF_2 and 2 m wireless FSO links, respectively.

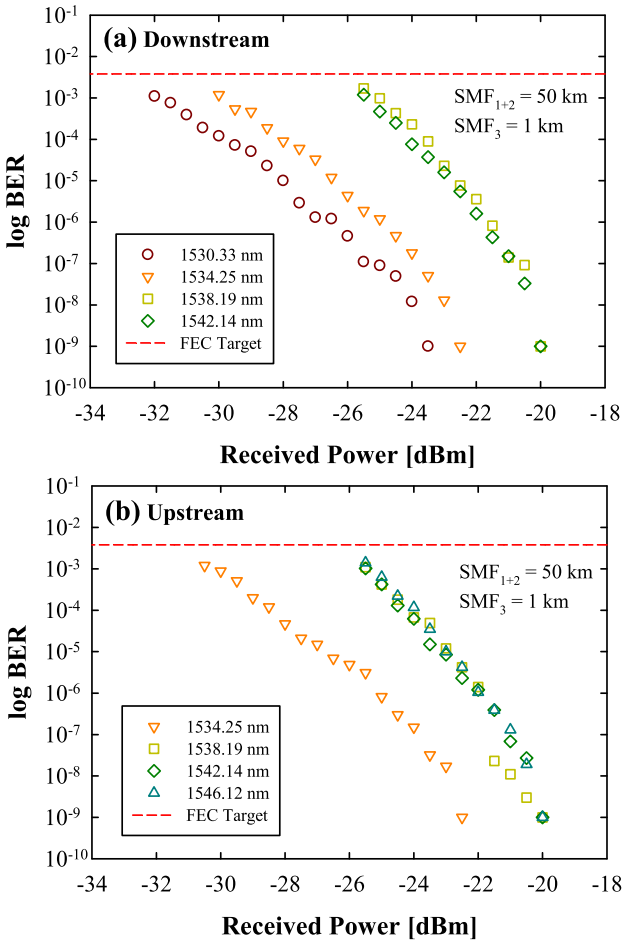

FIGURE 6. Obtained BER performances of four WDM (a) downstream and (b) upstream signals through 50 km $SMF_1 + SMF_2$, 1 km SMF_2 and 2 m FSO transmissions, respectively.

wavelengths after 50 km $SMF_1 + SMF_2$, 1 km SMF_2 and 2 m wireless FSO transmissions, respectively. The detected power sensitivities of four downstream signals are −32, −30, −25.5 and −25.5 dBm, respectively, as seen in Fig. 6(a), when the BER is below 3.8×10^{-3}. Furthermore, Fig. 6(b) exhibits the measured BER performance of upstream signal transmission. In this measurement, the corresponding sensitivities of −30.5, −25.5, −25.5 and −25.5 dBm are also attained below the FEC target, respectively. Hence, the total power budgets of the four downstream and upstream wavelengths are 39.5, 37.5, 33 and 33 dB, and 38, 33, 33 and 33 dB, respectively.

Next, we can estimate the total power budgets of the whole downstream signals based on the demonstrated WDM-FSO PON architecture of Fig. 2. The total insertion loss of the proposed access network is nearly 24.8 dB, including a WDM multiplexer (6 dB), 51 km SMF (10.2 dB), three OCs (2 dB), a 1 × 2 CP (3 dB) and FSO coupling loss (2.6 dB), respectively. Moreover, to confirm the longest FSO transmission length in the proposed access network, we can simulate the divergence loss at the pure atmosphere based on the designed FSO system by using the *TracePro* software. Here, the related operation parameters of FC and focusing lens between two OWUs are the same as above experimental setup. As seen in the red diamond of Fig. 7, the simulated FSO powers are obtained at the focal point of doublet lens between −8 and 6.4 dBm/mm^2 through the free space transmission lengths of 20 to 1000 m. As the FSO link length increases, the laser beam would diverge gradually. According to the simulation result, the beam divergence diameter of 0.7 to 28.7 cm is also obtained at the FSO connection length of 0 to 1000 m. When the FSO length is 400, 500, 760, 840, 880 and 940 m, the divergence diameter is observed at 11.9, 14.1, 22.0, 24.2, 25.3 and 27.0 cm, respectively. Fig. 7 also displays the corresponding divergence loss under different FSO length, when the atmospheric interferences of fog, rain, and turbulence are ignored. Therefore, the simulated divergence loss of 1.1 and 15.5 dB can be observed between two OWUs in the proposed FSO system through the FSO length of 20 to 1000 m, as seen in the black circle of Fig. 7. In the experiment and simulation, we only employ 50.4 mm diameter doublet lens to collect and enhance the diverged FSO power. To increase the detected

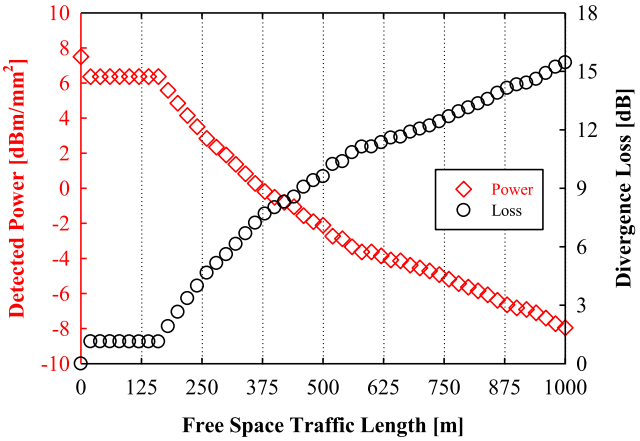

FIGURE 7. Simulation results of detected FSO power and corresponding divergence loss between two OWUs under different free space transmission length.

TABLE 1. Corresponding power budgets and insertion losses of four downstream WDM wavelengths in the proposed WDM FSO PON architecture, when the SMF_1 and SMF_2 are (a) 26 and 25 km and (b) 50 and 1 km, respectively.

(a) SMF_1+SMF_2 = 26 km; SMF_3 = 25 km

Wavelength (nm)	Total Power Budget (dB)	Insertion Loss (dB)	Redundant Budget (dB)	FSO Length (m)	Divergence Loss (dB)
1530.33	39	24.8	14.2	880	14.1
1534.25	38.5	24.8	13.7	840	13.6
1538.19	34.5	24.8	9.7	500	9.6
1542.14	34.5	24.8	9.7	500	9.6

(b) SMF_1+SMF_2 = 50 km; SMF_3 = 1 km

Wavelength (nm)	Total Power Budget (dB)	Insertion Loss (dB)	Redundant Budget (dB)	FSO Length (m)	Divergence Loss (dB)
1530.33	39.5	24.8	14.6	940	14.6
1534.25	37.5	24.8	12.7	760	12.7
1538.19	33	24.8	8.2	400	8.0
1542.14	33	24.8	8.2	400	8.0

divergence power, we could use a larger diameter lens in the proposed FSO system.

If we consider the weather conditions in the investigation. Tabs. 1(a) and 1(b) present the corresponding power budgets and insertion losses of four downstream WDM wavelengths in the proposed WDM-FSO PON architecture, when the SMF_1 + SMF_2 and SMF_2 are 26 and 25 km, and 50 and 1 km, respectively. Here, the total power budgets of four WDM-FSO signals are also shown in Tabs. 1(a) and 1(b), respectively. Based on the redundant power budget and corresponding divergence loss through various FSO transmission length, we can estimate the longest FSO transmission length of each downstream WDM wavelength. Therefore, the FSO transmission length of 400 to 940 m in the presented WDM-FSO PON can be supported, as seen in Tabs. 1(a) and 1(b). In this demonstration, we can select properly wavelength for the FSO connection based on different FSO transmission length without optical signal amplification. In addition, for the FSO upstream traffic, we can apply an optical amplifier in the OLT side to compensate the total upstream losses for demodulation. Hence, we do not need to consider the power budget for FSO upstream link.

Compared with the previous works [21], we only exploit two FCs with 20 mm diameter, a doublet lens with 50.4 mm diameter and an OC in each OWU for bidirectional FSO transmissions. The proposed geometric optics design of OWU could be integrated in cost-effective compact size for longer FSO wireless transmission under precise alignment. The proposed hybrid WDM FSO network architecture is not only simple, but also can avoid the RB beat noise. Here, we do not utilize the optical amplifier to compensate the insertion losses induced by other components for long-reach SMF and wireless FSO transmission based on the obtained power budget. Furthermore, the haze- and rain-induced atmospheric attenuations of FSO system have been demonstrated and analyzed in [22]. If the atmospheric state is light-haze, heavy-haze, light-rain and heavy-rain, respectively, the observed attenuation would be 0.61, 2.62, 6.8 and 19.77 dB/km. The atmospheric turbulence and misalignment are also the factors to cause the attenuation of FSO power [13], [23]. Therefore, an optical amplifier could be applied in a properly location to compensate the attenuation and increase the power budget for practical FSO transmission.

III. CONCLUSION

In summary, we demonstrated a bidirectional WDM-FSO PON system together with RB noise mitigation through 51 km long-reach SMF transmission. In the experiment, 4 × 10 Gbit/s OOK downstream (λ_1 to λ_4) and upstream signals (λ_2 to λ_5) were applied for data transmission. After 25 km SMF_1 and 26 km SMF_2 transmissions, and 2 m free space link length, the measured downstream and upstream power sensitivities were −32.5, −31, −27 and −27 dBm and −31, −26.5, −27 and −26.5 dBm, respectively, under the FEC target (BER $\leq 3.8 \times 10^{-3}$). When the SMF_1 and SMF_2 length changed to 50 and 1 km, respectively, the obtained power sensitivities were −32, −30, −25.5 and −25.5 dBm and −30.5, −25.5, −25.5 and −25.5 dBm. Here, to determine the longest FSO transmission length in the proposed PON system, we could simulate the corresponding optical parameters for demonstration by utilizing the *TracePro* software. Based on the experimental and simulated results, the free space transmission length of the proposed WDM network without signal amplification could be reached from 400 to 940 m according to the different FSO wavelengths. In addition, to extend the FSO transmission length in the proposed WDM-FSO access network, we could use an optical amplifier in the corresponding OWU to compensate the whole insertion losses.

REFERENCES

[1] H.-Y. Wang, C.-H. Cheng, C.-T. Tsai, Y.-C. Chi, and G.-R. Lin, "28-GHz wireless carrier heterodyned from orthogonally polarized tri-color laser diode for fading-free long-reach MMWoF," *J. Lightw. Technol.*, vol. 37, no. 13, pp. 3388–3400, Jul. 1, 2019.

[2] C.-H. Yeh, C.-W. Chow, H.-Y. Chen, and B.-W. Chen, "Using adaptive four-band OFDM modulation with 40 Gb/s downstream and 10 Gb/s upstream signals for next generation long-reach PON," *Opt. Express*, vol. 19, no. 27, pp. 26150–26160, 2011.
[3] C.-Y. Li, H.-W. Wu, H.-H. Lu, W.-S. Tsai, S.-E. Tsai, and J.-Y. Xie, "A hybrid Internet/CATV/5G fiber-FSO integrated system with a triple-wavelength polarization multiplexing scenario," *IEEE Access*, vol. 7, pp. 151023–151033, 2019.
[4] M.-Y. Huang, Y.-W. Chen, P.-C. Peng, H. Wang, and G.-K. Chang, "A full field-of-view self-steering beamformer for 5G mm-wave fiber-wireless mobile fronthaul," *J. Lightw. Technol.*, vol. 38, no. 6, pp. 1221–1229, Mar. 15, 2020.
[5] C.-H. Yeh, C.-W. Chow, C.-H. Wang, Y.-F. Wu, F.-Y. Shih, and S. Chi, "Using OOK modulation for symmetric 40-Gb/s long-reach time-sharing passive optical networks," *IEEE Photon. Technol. Lett.*, vol. 22, no. 9, pp. 619–621, May 1 2010.
[6] R. Gaudino, S. Capriata, and V. Curri, "Propagation impairments due to Raman effect on the coexistence of GPON, XG-PON, RF-video and TWDM-PON," in *Proc. 39th Eur. Conf. Exhib. Opt. Commun. (ECOC)*, 2013, pp. 1–3.
[7] F.-Y. Shih, C.-H. Yeh, C.-W. Chow, C.-H. Wang, and S. Chi, "Utilization of self-injection Fabry–Pérot laser diode for long-reach WDM-PON," *Opt. Fiber Technol.*, vol. 16, no. 1, pp. 46–49, 2010.
[8] M. Zhu, L. Zhang, S.-H. Fan, C. Su, G. Gu, and G.-K. Chang, "Efficient delivery of integrated wired and wireless services in UDWDM-RoF-PON coherent access network," *IEEE Photon. Technol. Lett.*, vol. 24, no. 13, pp. 1127–1129, Jul. 1, 2013.
[9] L. Yi, Z. Li, M. Bi, W. Wei, and W. Hu, "Symmetric 40-Gb/s TWDM-PON with 39-dB power budget," *IEEE Photon. Technol. Lett.*, vol. 25, no. 7, pp. 644–647, Apr. 1, 2013.
[10] K. Taguchi, K. Asaka, S. Kimura, K.-I. Suzuki, and A. Otaka, "Reverse bias voltage controlled burst-mode booster SOA in λ-tunable ONU transmitter for high-split-number TWDM-PON," *J. Opt. Commun. Netw.*, vol. 10, no. 4, pp. 431–439, 2018.
[11] D. Fujimoto, H.-H. Lu, K. Kumamoto, S.-E. Tsai, Q.-P. Huang, and J.-Y. Xie, "Phase-modulated hybrid high-speed Internet/WiFi/Pre-5G in-building networks over SMF and PCF with GI-POF/IVLLC transport," *IEEE Access*, vol. 7, pp. 90620–90629, 2019.
[12] C.-H. Yeh, W.-P. Lin, C.-M. Luo, Y.-R. Xie, Y.-J. Chang, and C.-W. Chow, "Utilizing single lightwave for delivering baseband/FSO/MMW traffics simultaneously in PON architecture," *IEEE Access*, vol. 7, pp. 138927–138931, 2019.
[13] J. Zhang, J. Wang, Y. Xu, M. Xu, F. Lu, L. Cheng, J. Yu, and G.-K. Chang, "Fiber-wireless integrated mobile backhaul network based on a hybrid millimeter-wave and free-space-optics architecture with an adaptive diversity combining technique," *Opt. Lett.*, vol. 41, no. 9, pp. 1909–1912, 2016.
[14] W.-S. Tsai, H.-H. Lu, Y.-C. Huang, S.-C. Tu, and Q.-P. Huang, "A PDM-based bi-directional fibre-FSO integration with two RSOAs scheme," *Sci. Rep.*, vol. 9, no. 1, pp. 1–8, Dec. 2019.
[15] R. Zhang, F. Lu, M. Xu, S. Liu, P.-C. Peng, S. Shen, J. He, H. J. Cho, Q. Zhou, S. Yao, and G.-K. Chang, "An ultra-reliable MMW/FSO A-RoF system based on coordinated mapping and combining technique for 5G and beyond mobile fronthaul," *J. Lightw. Technol.*, vol. 36, no. 20, pp. 4952–4959, Oct. 15, 2018.
[16] M. Patel, A. Darji, D. Patel, and U. Dalal, "Mitigation of RB noise in bidirectional fiber transmission systems based on different OFDM SSB techniques," *Opt. Commun.*, vol. 426, pp. 273–277, Nov. 2018.
[17] A. Chowdhury, H.-C. Chien, M.-F. Huang, J. Yu, G.-K. Chang, "Rayleigh backscattering noise-eliminated 115-km long-reach bidirectional centralized WDM-PON with 10-Gb/s DPSK downstream and remodulated 2.5-Gb/s OCS-SCM upstream signal," *IEEE Photon. Technol. Lett.*, vol. 20, no. 24, pp. 2081–2083, Dec. 15, 2008.
[18] C.-H. Yeh, C.-W. Chow, and L.-Y. Wei, "Symmetric >67 Gbps OFDM-IMDD based WDM access network for mitigating Rayleigh backscattering interference noise," *Opt. Commun.*, vol. 454, Jan. 2020, Art. no. 124504.
[19] H. Yao, W. Li, Q. Feng, J. Han, Z. Ye, Q. Hu, Q. Yang, and S. Yu, "Ring-based colorless WDM-PON with Rayleigh backscattering noise mitigation," *J. Opt. Commun. Netw.*, vol. 9, no. 1, pp. 27–35, 2017.
[20] C. H. Yeh, C. W. Chow, S. P. Huang, J. Y. Sung, Y. L. Liu, and C. L. Pan, "Ring-based WDM access network providing both Rayleigh backscattering noise mitigation and fiber-fault protection," *J. Lightw. Technol.*, vol. 30, no. 20, pp. 3211–3218, Oct. 15, 2012.
[21] H.-W. Wu, H.-H. Lu, W.-S. Tsai, Y.-C. Huang, J.-Y. Xie, Q.-P. Huang, and S.-C. Tu, "A 448-Gb/s PAM4 FSO communication with polarization-multiplexing injection-locked VCSELs through 600 m free-space link," *IEEE Access*, vol. 8, pp. 28859–28866, 2020.
[22] G. Kaur and H. Singh, "Design & investigation of 32×10 Gbps DWDM-FSO link under different weather condition," *Int. J. Adv. Res. Comput. Sci.*, vol. 8, no. 4, pp. 79–82, 2017.
[23] T. Joseph, H. Kaushal, V. K. Jain, and S. Kar, "Performance analysis of OOK modulation scheme with spatial diversity in atmospheric turbulence," in *Proc. 23rd Wireless Opt. Commun. Conf. (WOCC)*, May 2014, pp. 1–3, Paper O3.5.

CHIEN-HUNG YEH received the Ph.D. degree from the Institute of Electro-Optical Engineering, National Chiao Tung University, Taiwan, in 2004. In 2004, he joined the Information and Communications Research Laboratories (ICL), Industrial Technology Research Institute (ITRI), Taiwan, as a Researcher, where he was promoted to a Principal Researcher for leading the ITRI Industrial-Academic Projects, in 2008. In 2014, he joined the Faculty of Department of Photonics, Feng Chia University, Taiwan, where he is currently a Professor. His research interests include optical fiber communication, fiber lasers and amplifiers, PON access, MMW communication, fiber sensors, and VLC and FSO-based Li-Fi communications.

JHAO-REN CHEN received the B.S. degree from the Department of Physics, Tunghai University, Taiwan, in 2019. He is currently pursuing the M.S. degree with the Department of Photonics, Feng Chia University, Taiwan.

WEI-YAO YOU received the B.S. degree from the Department of Photonics, Feng Chia University, Taiwan, in 2019, where he is currently pursuing the M.S. degree with the Department of Photonics.

CHI-WAI CHOW (Senior Member, IEEE) received the B.Eng. (Hons.) and Ph.D. degrees from the Department of Electronics Engineering, The Chinese University of Hong Kong (CUHK), in 2001 and 2004, respectively. His Ph.D. thesis was focused on optical packet-switched networks. He was appointed as a Postdoctoral Fellow of the CUHK, involved in silicon photonics. From 2005 to 2007, he was a Postdoctoral Research Scientist, involved mainly in two European Union projects, such as Photonic Integrated Extended Metro and Access Network (PIEMAN) and Transparent Ring Interconnection Using Multi-Wavelength Photonic Switches (TRIUMPH), with the Department of Physics, Tyndall National Institute, University College Cork, Ireland. In 2007, he joined the Department of Photonics, National Chiao Tung University, Taiwan, where he is currently a Professor.